Journal of Materials Chemistry B

Accepted Manuscript

ROYAL SOCIETY OF CHEMISTRY

www.rsc.org/materialsB

Journal Name

RSCPublishing

ARTICLE

Fluorescent light-up probe with "AIE + ESIPT" characteristics for specific detection of lysosomal esterase

Cite this: DOI: 10.1039/x0xx00000x

Received 00th January 2012,
Accepted 00th January 2012

DOI: 10.1039/x0xx00000x

www.rsc.org/

Meng Gao,□[a] Qinglian Hu,□[b] Guangxue Feng,[b] Ben Zhong Tang,[c,d] Bin Liu*[a,b]

We report a fluorescent light-up probe **AIE-Lyso-1** for *in situ* visualization of lysosomal esterase activity. The probe is based on a salicyladazine fluorogen, which is conjugated with esterase reactive acetoxyl groups and lysosome-targeting morpholine moieties. The probe has characteristics of both aggregation-induced emission (AIE) and excited-state intramolecular proton transfer (ESIPT), which shows significant advantages, such as lysosome-specific targeting, no self-quenching at high concentration, excellent light-up ratio, large Stokes shift, low cytotoxicity, and high specifity to esterase. It has also been used for *in situ* monitoring of lysosomal esterase activity and tracking lysosomal movements in living cells, which has great potentials for the diagnosis of Wolman disease caused by deficiency of lysosomal esterase.

Introduction

Lysosomal enzymes are responsible for intracellular digestion of various proteins, lipids, and carbohydrates, and their functional deficiencies would lead to a number of inherited lysosomal storage disorders (LSDs).[1] For example, the deficiency of lysosomal esterase would result in Wolman disease with a series of symptoms including diarrhea, swelling of the abdomen, enlargement of the liver and failure to gain weight.[2] Because the early diagnosis and therapy is critical for treatment of lysosomal storage disorders, a high-throughput assay has been established for the newborn screening of a subset of LSDs *via* LC-MS analysis of cell extracts.[3] However, the LC-MS method requires complicated procedures for sample preparation and is not able to *in situ* monitor enzyme activities. As compared with the LC-MS method, fluorescence based detection shows unique advantages in sensitivity, spatial and temporal resolution, as well as *in situ* visulization of biological processes.[4] In the past few years, although various esterase-sensitive fluorescent probes have been developed based on fluoresceines, resorufins, and BODIPYs,[5] they are not able to be specifically localized in lysosomes to provide *in situ* information on lysosomal esterase activity. Moreover, the accumulation of fluorogens in lysosomes always leads to high local concentration, which naturally results in fluorogen self-quenching with low fluorescence.[6] These probes also suffer from other disadvantages, such as easy diffusion away from reactive sites and small Stokes shift (< 40 nm). Despite of some initial efforts made toward the lysosomal esterase activity study,[5m] there is no detailed report of the probe design and performance evaluation in the literature. It is highly desirable to develop self-quenching free and light-up probes for real-time monitoring of enzyme activity in specifc organelles of living cells.

The discovery of fluorogens with aggregation induced emission (AIE) characteristics has opened new opportunities to develop light-up probes for specific enzyme detection.[7] These AIE fluorogens are highly emissive in aggregation state but remain very weakly fluorescent in dilute solution. This is due to the restriction of intramolecular motion of AIE fluorogens in aggregation state and rapid intramolecular motion in solution.[7a]

[a] *Institute of Materials Research Engineering, 3 Research Link, Singapore 117602*

[b] *Department of Chemical and Biomolecular Engineering, 4 Engineering Drive 4, National University of Singapore, Singapore 117585*

[c] *Department of Chemistry, Institute for Advanced Study, Division of Biomedical Engineering, State Key Laboratory of Molecular Neuroscience and Institute of Molecular Functional Materials, The Hong Kong University of Science and Technology, Clear Water Bay, Kowloon, Hong Kong, China*

[d] *SCUT-HKUST Joint Research Laboratory, Guangdong Innovative Research Team, State Key Laboratory of Luminescent Materials & Devices, South China University of Technology, Guangzhou 510640, China*

† Electronic supplementary information (ESI) available: Experimental procedures, structural characterization data. For ESI See DOI: 10.1039/b000000x

□These authors contributed equally to this work.

The AIE probes offer significant advantages in high signal-to-noise ratio and excellent photostability.[8] However, the first generation of enzyme specific AIE probes requires very high water-solubility to ensure low background signal, which limits the AIE fluorogens to be only conjugated with very hydrophilic substrates.[8a] To overcome this limitation, we propose a novel fluorescent light-up probe design by combining AIE and excited state intramolecular proton transfer (ESIPT) mechanism. As fluorogens with ESIPT mechanism rely on intramolecular hydrogen bonding to induce fluorescence change, blocking of the excited-state proton transfer from a proton donor (usually hydroxyl or amino group) to an acceptor atom (oxygen or nitrogen) can easily lead to fluorogens in the dark state or change in emission wavelengths.[9] Substitution of specific enzyme substrate to the hydroxyl or amino groups thus could lead to ratiometric or light-up probes after deprotection of the protected hydroxyl groups. In this regard, both hydrophobic and hydrophilic substrates could be used for enzyme detection as the fluorescence change is controlled by hydrogen bonding rather than water-solubility of the probe. It's noteworthy that the high polarity and hydrogen-bond donor ability of solvents would inhibit the ESIPT emission with large Stokes shift,[10] but the AIE characteristics could favor the ESIPT emission by formation of aggregates, which is benefical for improving the detection sensitivity with high signal to noise ratio. Based on these considerations, in this contribution, an "AIE + ESIPT" probe **AIE-Lyso-1** is designed by conjugation of the salicyladazine fluorophore[11] with esterase reactive acetoxyl groups and lysosome-targeting morpholines[12] (Scheme 1). The blocking of hydroxyl groups with acetyl groups is able to quench the salicyladazine fluorescence, due to the destroying of hydrogen bonding and the free rotating of the *N*–*N* bond. After reaction with esterase to cleave the acetyl groups, the corresponding product **2** would light-up by intramolecular hydrogen bonds formation to activate ESIPT process and aggregation in aqueous media to activate AIE process. As compared to the previous AIE or ESIPT probes, the "AIE + ESIPT" probes do not limit to hydrophilic substrates and favor the emission with large Stokes shift, which offers a more general platform for designing light-up probes for biological sensing. The simple probe design together with the easy modification also makes it possible to develop specific probes for targeted imaging, e.g. in this case, the morpholine groups are added to ensure the targeting of the probe to lysosome.

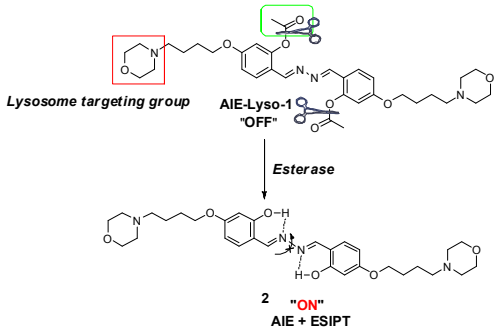

Scheme 1 Design of probe **AIE-Lyso-1** for specific detection of lysosomal esterase.

Results and discussion

Synthesis of probes

AIE-Lyso-1 was synthesized in 42% overall yield according to the synthetic procedure shown in Scheme 2. The reaction between 2,4-dihydroxybenzaldehyde **3** and 1,4-dibromobutane first formed compound **4** in 65% yield, which further reacted with hydrazine hydrate to produce the salicyladazine compound **5** in 80% yield. Compound **5** was further reacted with morpholine and acetic anhydride to finally afford the desired product **AIE-Lyso-1** in 81% yield. The NMR and mass spectroscopy confirmed the right molecular structures (see SI for details). As a control, probe **6** without lysosome targeting morpholine groups was synthesized in 86% yield from compound **5** and acetic anhydride.

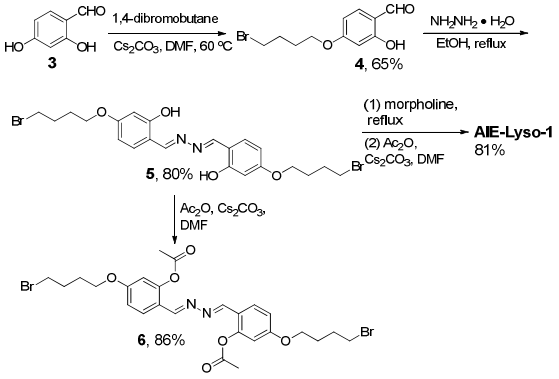

Scheme 2 Synthetic routes to probes **AIE-Lyso-1** and **6**.

Optical properties

Fig. 1 shows the UV and photoluminescence (PL) spectra of **AIE-Lyso-1** and the esterase reaction product **2**. **AIE-Lyso-1** shows an absorption maximum at 333 nm, with negligible fluorescence at ~532 nm. At the same concentration of 10 μM, the absorption maximum of fluorogen **2** is red-shifted to 356 nm, with a strong emission at ~532 nm, which is 200-fold higher as compared to that for **AIE-Lyso-1**. The red-shifted absorption of **2** is ascribed to its increased planarity and rigidity by forming of intramolecular hydrogen bonds. It's also noteworthy that there is almost no overlap

between the absorption and emission spectra for **2**. The large Stokes shift (176 nm) for **2** is highly desirable for bioimaging applications.

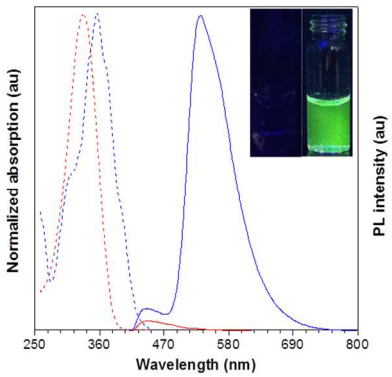

Fig. 1 UV−vis absorption (dashed line) and PL (solid line) spectra of **AIE-Lyso-1** (red) and **2** (blue) in DMSO/water (1:99 v/v). Inset: Photographs of **AIE-Lyso-1** (left) and **2** (right) in DMSO/water (1:99 v/v) taken under UV irradiation. λ_{ex} = 356 nm. [**AIE-Lyso-1**] = [**2**] = 10 μM.

The PL spectra of **2** were studied in THF/water mixtures with different water fractions (f_w), which enabled fine-tuning of the solvent polarity and the extent of solute aggregation (Fig. 2). **2** in pure THF solution shows weak green fluorescence with an emission maximum at 532 nm. With gradual addition of water into THF from f_w = 0 to 80 vol%, the emission intensity keeps increasing slowly. From f_w = 80 to 99 vol%, the emission is exponentially increased with formation of aggregates due to the poor solubility of **2** in aqueous media (see Fig. S1). At f_w = 99 vol%, a 14-fold enhancement of emission was observed as compared to that in THF, revealing an obvious AIE effect.

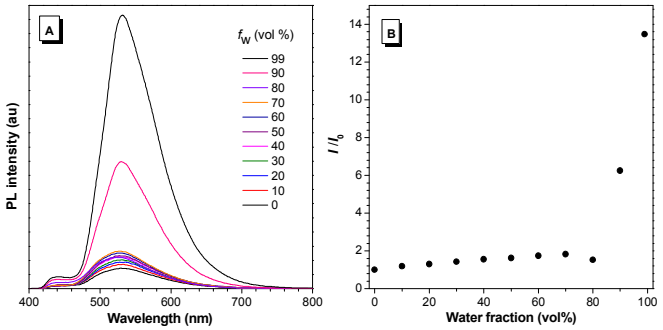

Fig. 2 (A) PL spectra of **2** in THF and THF/water mixtures with different water fractions (f_w); [2] = 10 μM; λ_{ex} = 356 nm. (B) Plot of relative PL intensity (I/I_0) versus the solvent composition of THF/water mixture of **2**.

Study of esterase activities in solution

Fig. 3 depicts the fluorescence kinetic curve of **AIE-Lyso-1** upon incubation with esterase at different concentrations. As shown in Fig. 3A, higher concentrations of esterase result in faster cleavage and stronger fluorescence intensity. For esterase at 0.50 U mL^{-1}, the fluorescence increase reaches a plateau in 15 min, which is sigmoidal in shape due to the two-stepwise sequential hydrolysis of **AIE-Lyso-1** to **2**. In contrast, the fluorescence of **AIE-Lyso-1** without esterase hardly changes during the same period of time, indicating good stability of the probe. As shown in Fig. 3B, a good linearity is found in the esterase concentration range of 0.10–0.50 U mL^{-1}, with a linear equation of $F = 0.416 \times 10^3 \times C$ (U mL^{-1}) + 0.80 (γ = 0.991). The detection limit (3S/m, in which S is the standard deviation of blank measurements, and m is the slope of the linear equation) is determined to be 2.4 × 10^{-3} U mL^{-1}. The fluorescence response of **AIE-Lyso-1** at varied concentrations (0–10 μM) was also investigated with 0.50 U mL^{-1} esterase (see Fig. S2), and increasing fluorescence intensity was observed with higher probe concentration.

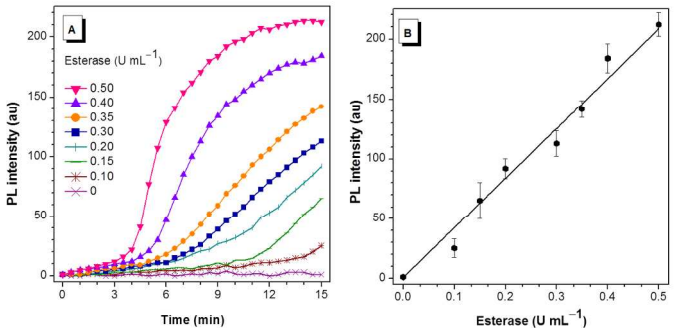

Fig. 3 (A) A plot of fluorescence intensity of **AIE-Lyso-1** (10 μM) vs. the reaction time at esterase concentrations (from bottom to top): 0 (control), 0.10, 0.15, 0.20, 0.30, 0.35, 0.40 and 0.50 U mL^{-1}. (B) The plot of the fluorescence intensity against the esterase concentration in the range of 0–0.50 U mL^{-1}. The measurements were performed in 10 mM PBS (pH 7.4) with $\lambda_{ex/em}$ = 356/532 nm.

The selectivity of **AIE-Lyso-1** towards esterase was then evaluated by measuring its fluorescence response in the presence of different interference substances (Fig. 4), including inorganic salts ($MgCl_2$, $CaCl_2$), vitamin C, reactive oxygen species (H_2O_2, BO_3^-),[13] and proteins (lysozyme, cathepsin B). The esterase can induce over 70–200 folds fluorescence enhancements than other interference substances, which demonstrate that **AIE-Lyso-1** has high selectivity for esterase.

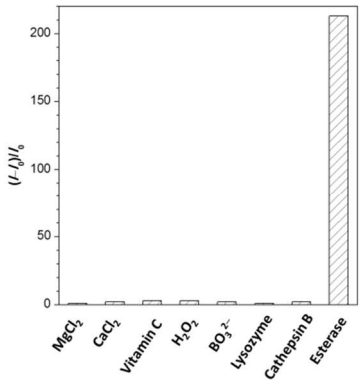

Fig. 4 Fluorescence responses of **AIE-Lyso-1** (10 μM) to various species: $MgCl_2$ (100μM), $CaCl_2$ (100 μM), vitamin C (10 mM), H_2O_2 (100 μM), BO_3^- (100 μM), Lysozyme (1.0 U mL^{-1}), Cathepsin B (1.0 U mL^{-1}), and esterase (0.50 U mL^{-1}) in PBS buffer solution (pH = 7.4, 37 °C) with $\lambda_{ex/em}$ = 356/532, where I_0 and I are the PL intensities of 10 μM **AIE-Lyso-1** alone and that upon incubation with different species, respectively.

To further confirm that the fluorescence light-up was caused by esterase, we also investigated the inhibition effect of 4-(2-aminoethyl)benzenesulfonyl fluoride (AIEBSF) on esterase activity. As shown in Fig. 5, with increasing AIEBSF concentration, the fluorescence intensity of **AIE-Lyso-1** at 532 nm is gradually

decreased. For example, addition of 0.1 mM AIEBSF causes a 10% decrease of the original fluorescence intensity. The higher concentrations of AIEBSF such as 0.4 and 1.0 mM lead to 40% and 65% decrease of the original fluorescence intensity, respectively. These results further confirm that the light-up fluorescence indeed arises from the reaction of probe **AIE-Lyso-1** with esterase. **AIE-Lyso-1** can also be used to monitor the inhibition effect of AIEBSF in living cells. When MCF-7 cells were pretreated with 0.4 mM AIEBSF, an obviously decreased fluorescence was observed (see Fig. S3).

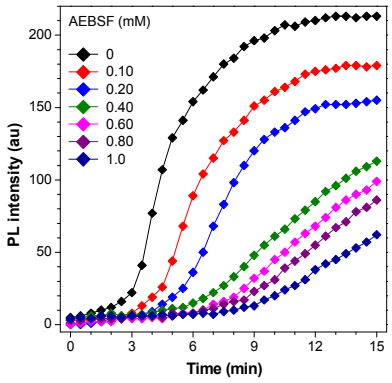

Fig. 5 The fluorescence change of **AIE-Lyso-1** (10 μM) upon incubation with esterase (0.50 U mL^{-1}) as a function of time in the presence of different concentrations of AIEBSF (from top to bottom): 0, 0.10, 0.20, 0.40, 0.60, 0.80 and 1.0 mM. $\lambda_{ex/em}$ = 356/532 nm.

Cell imaging

After investigating **AIE-Lyso-1** as an esterase probe in solution, we further explored its application for imaging of lysosomal esterase in living MCF-7 cells. After incubation with 1 μM **AIE-Lyso-1** for 30 min (Fig. 6b), a discrete labeling pattern that matches the distribution of lysosomes is obtained, which overlaps well with the LysoTracker Red costaining (Fig. 6c–d), suggesting the high specificity of **AIE-Lyso-1** for lysosomes. To verify that morpholine groups play an important role in selective targeting lysosomes, probe **6** without morpholine groups was also tested. Because of the low cell membrane permeability of **6**, very weak fluorescence is observed for cells incubated with 1.0 μM **6** for 2 h (see Fig. S4); while a non-specific staining of the entire cell cytoplasm is observed upon incubation the cells with 5.0 μM **6** (Fig. 6e–h) for 2 h. These experiments clearly verified that **AIE-Lyso-1** could selectively target lysosomes with high cell membrane permeability. The photostability of **AIE-Lyso-1** and LysoTracker Red was also tested through continuous laser scanning by confocal microscope, which shows that the signal loss of **AIE-Lyso-1** is less than 20% in ~ 8 min (See Fig. S5). In contrast, LysoTracker Red lost almost ~70% of its fluorescence signal within the same period of time. These experiments demonstrate that **AIE-Lyso-1** has very good photostability. Cytotoxicity of **AIE-Lyso-1** was also evaluated by the widely used MTT assay. The samples were incubated with 1, 2, 4, 8, or 16 μM **AIE-Lyso-1** for 24 h, and the cell viabilities were close to 100% under the testing conditions, indicating the low cytotoxicity of the probe (see Fig. S6).

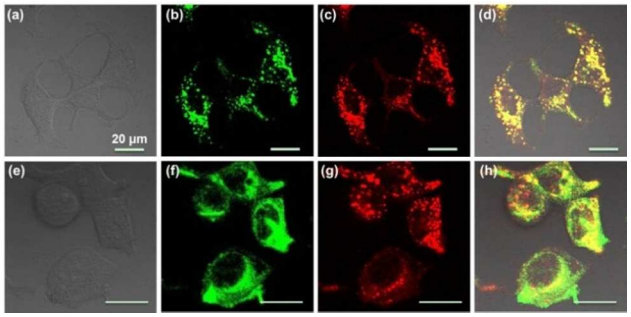

Fig. 6 (a–d) Confocal images of MCF-7 cells stained with 1.0 μM **AIE-Lyso-1** and 50 nM LysoTracker Red: (a) Bright-field image; (b) Confocal image from **AIE-Lyso-1** on channel 1 (λ_{ex} = 405 nm, λ_{em} = 515−560 nm); (c) Confocal image from LysoTracker Red on channel 2 (λ_{ex} = 559 nm, λ_{em} = 585−610 nm); (d) The overlay of (b) and (c). (e–f) Confocal images of MCF-7 cells stained with 5.0 μM **6** and 50 nM LysoTracker Red: (e) Bright-field image; (f) Confocal image from **6** on channel 1; (g) Confocal image from LysoTracker Red on channel 2; (h) The overlay of (f) and (g). Scale bar = 20 μm.

To explore whether **AIE-Lyso-1** can be used for *in situ* monitoring of lysosomal esterase activity, real-time imaging experiments were performed with MCF-7 cells (Fig. 7). As the incubation time elapses, the fluorescence intensity in lysosome increases quickly and reaches a maximum at ~8 min, meanwhile no fluorescence was observed in the culture media. In comparison, probe **6** without lysosome targeting group can only light-up the entire cell after 2 h (see S6). These results demonstrate that **AIE-Lyso-1** has the ability for specifical targeting lysosome and real-time monitoring of lsysosomal esterase activity.

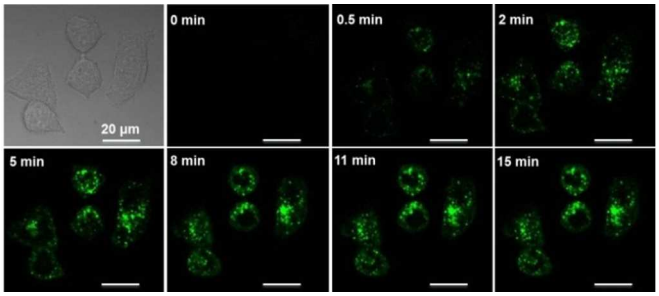

Fig. 7 Real-time fluorescence images showing the **AIE-Lyso-1** (1.0 μM) stained MCF-7 cells at room temperature. Scale bar = 20 μm.

As the spatial and temporal distribution of lysosomes can also help to diagnose the lysosomal storage diseases,[14] **AIE-Lyso-1** was further used for tracking lysosomal movements (Fig. 8). The cells were stimulated by 3 μM of chloroquine, which can drive lysosomal movements without inducing significant disturbance. The movements of lysosomes were subsequently monitored continually by confocal microscopy. As shown in Fig. 8, even the slight movement of lysosomes could be identified by **AIE-Lyso-1** in the merged images (Fig. 8e–g) collected at different times.

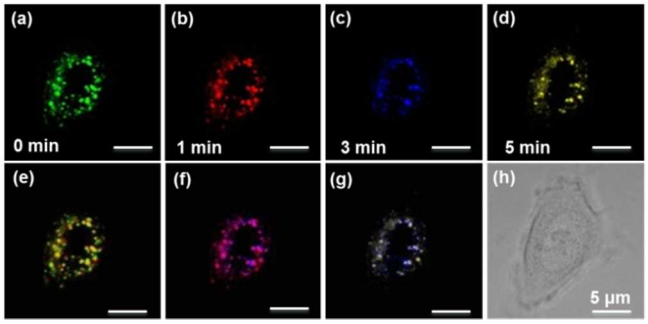

Fig. 8 Confocal images of an MCF-7 cell stained with 1.0 μM **AIE-Lyso-1** and stimulated using 3 μM chloroquine. Different pseudo-colors are used to illustrate the fluorescence images at different stimulation times of 0, 1, 3, and 5 min. (e−g) Merging images at two different times: (e) 0 and 1 min, (f) 1 and 3 min, (g) 3 and 5 min, and (h) Bright-field image. Scale bar = 5 μm.

Conclusions

In summary, a novel fluorescent light-up probe **AIE-Lyso-1** with "AIE + ESIPT" characteristics has been developed for specific detection of lysosomal esterase activity in living cells, which has also been used for monitoring the lysosomal movements. Compared with the reported esterase probes, **AIE-Lyso-1** has significant advantages in lysosome-specific targeting, no self-quenching at high concentration, excellent light-up ratio, large Stokes shift, good photostability, and low cytotoxicity. The unique and simple design also overcomes the limitations of the previously reported AIE light-up probes, e.g. high water-solubility of the probe is no longer a perquisite to ensure low background fluorescence. It also favors the ESIPT emission with large Stokes shift by formation of aggregates to prevent from the interruption of water's high polarity and hydrogen-bond donor ability. The strategy presented herein can be easily extended for designing "AIE + ESIPT" light-up probes for specific detection of various enzymes and other analytes simply through conjugation of cleavable recognition elements to the "AIE + ESIPT" fluorogen. Further fine-tuning of the molecular structures will likely to yield long wavelength emissive "AIE + ESIPT" fluorogens for real-time *in vivo* imaging applications.

Acknowledgements

We thank the Singapore National Research Foundation (R-279-000-390-281), the SMART (R279-000-378-592), Institute of Materials Research and Engineering (IMRE/12-8P1103), the Research Grants Council of Hong Kong (HKUST2/CRF/10 and N_HKUST620/11) and Guangdong Innovative Research Team Program (201101C0105067115) for finantial support.

Notes and references

1. A. Vellodi, *Br. J. Haematol.*, 2005, **128**, 413–431.
2. R. A. Anderson, R. S. Byrum, P. M. Coates and G. N. Sando, *Proc. Natl. Acad. Sci. U.S.A.*, 1994, **91**, 2718–2722.
3. (a) Z. Spacil, H. Tatipaka, M. Barcenas, C. R. Scott, F. Turecek and M. H. Gelb, *Clin. Chem.*, 2013, **59**, 502–511; (b) Y. Li, C. R. Scott, N. A. Chamoles, A. Ghavami, B. M. Pinto, F. Turecek and M. H. Gelb, *Clin. Chem.*, 2004, **50**, 1785–1796.
4. (a) A. Baruch, D. A. Jeffery and M. Bogyo, *Trends Cell Biol.*, 2004, **14**, 29–35; (b) 1. M. D. Witte, W. W. Kallemeijn, J. Aten, K. Y. Li, A. Strijland, W. E. Donker–Koopman, A. M. van den Nieuwendijk, B. Bleijlevens, G. Kramer, B. I. Florea, B. Hooibrink, C. E. Hollak, R. Ottenhoff, R. G. Boot, G. A. van der Marel, H. S. Overkleeft and J. M. AIErts, *Nat. Chem. Biol.*, 2010, **6**, 907–913.
5. (a) E. Nakata, Y. Yukimachi, Y. Nazumi, Y. Uto, T. Hashimoto, Y. Okamoto and H. Hori, *Chem. Lett.*, 2010, 39, 734–735; (b) G. Zlokarnik, *Science*, 1998, **279**, 84–88; (c) W. H. t. Humphries and C. K. Payne, *Anal. Biochem.*, 2012, **424**, 178–183; (d) R. Sicart, M. P. Collin and J. L. Reymond, *Biotechnol. J.*, 2007, **2**, 221–231; (e) Y. Yang, P. Babiak and J. L. Reymond, *Org. Biomol. Chem.*, 2006, **4**, 1746–1754; (f) L. D. Lavis, T. Y. Chao and R. T. Raines, *Chem. Sci.*, 2011, **2**, 521–530; (g) Y. Kim, Y. Choi, R. Weissleder and C. H. Tung, *Bioorg. Med. Chem. Lett.*, 2007, **17**, 5054–5057; (h) N. Dai, Y. N. Teo and E. T. Kool, *Chem Commun.*, 2010, **46**, 1221–1223; (i) M. N. Levine, T. T. Hoang and R. .T. Raines, *Chem. Biol.*, 2013, **20**, 614–618; (j) S. D. Goldman, R. S. Funk, R. A. Rajewski and J. P. Krise, *Bioanal.*, 2009, **1**, 1445–1459; (k) T. Komatsu, Y. Urano, Y. Fujikawa, T. Kobayashi, H. Kojima, T. Terai, K. Hanaoka and T. Nagano, *Chem. Commun.*, 2009, 7015–7017; (l) Y. Zhang, W. Chen, D. Feng, W. Shi, X. Li and H. Ma, *Analyst*, 2012, **137**, 716–721; (m) J. J. Naleway, D. J. Coleman, A. P. Guzikowski and S. P. Williamson, *Faseb J.*, 2008, **22**, 1059.1.
6. V. Weissig and G. G. D'Souza, *Organelle–Specific Pharmaceutical Nanotechnology*, Wiley, 2011.
7. (a) Y. Hong, J. W. Lam and B. Z. Tang, *Chem. Soc. Rev.*, 2011, **40**, 5361–5388; (b) H. Shi, R. T. Kwok, J. Liu, B. Xing, B. Z. Tang and B. Liu, *J. Am. Chem. Soc.*, 2012, **134**, 17972–17981; (c) H. Shi, J. Liu, J. Geng, B. Z. Tang and B. Liu, *J. Am. Chem. Soc.*, 2012, **134**, 9569–9572; (d) X. Wang, H. Liu, J. Li, K. Ding, Z. Lv, Y. Yang, H. Chen and X. Li, *Chem. Asian. J.*, 2014, DOI: 10.1002/asia.201301326; (e) J. Liang, R. T. Kwok, H. Shi, B. Z. Tang and B. Liu, *ACS Appl. Mater. Interfaces*, 2013, **5**, 8784–8789; (f) X. Gu, G. Zhang, Z. Wang, W. Liu, L. Xiao and D. Zhang, *Analyst*, 2013, **138**, 2427–2431; (g) M. Wang, G. Zhang, D. Zhang, D. Zhu and B. Z. Tang, *J. Mater. Chem.* 2010, **20**, 1858–1867.
8. (a) D. Ding, K. Li, B. Liu and B. Z. Tang, *Acc. Chem. Res.*, 2013, **46**, 2441–2453; (b) C. W. Leung, Y. Hong, S. Chen, E. Zhao, J. W. Lam and B. Z. Tang, *J. Am. Chem. Soc.*, 2013, **135**, 62–65.
9. (a) Y. Xu, Q. Liu, B. Dou, B. Wright, J. Wang and Y. Pang, *Adv. Healthc. Mater.*, 2012, **1**, 485–492; (b) J. Zhao, S. Ji, Y. Chen, H. Guo and P. Yang, *Phys. Chem. Chem. Phys.*, 2012, **14**, 8803–8817. 1; (c) R. Hu, J. Feng, D. Hu, S. Wang, S. Li, Y. Li and G. Yang, *Angew. Chem. Int. Ed.*, 2010, **49**, 4915–4918; (d) T. I. Kim, H. J. Kang, G. Han, S. J. Chung and Y. Kim, *Chem. Commun.*, 2009, 5895–5897;
10. (a) A. Klymchenko, C. Kenfack, G. Duportail and Y. Mély, *J. Chem. Sci.*, 2007, **119**, 83–89; (b) K. Das, N. Sarkar, A. K. Ghosh, D. Majumdar, D. N. Nath and K. Bhattacharyya, *J. Phys. Chem.*, 1994, **98**, 9126–9132;
11. W. Tang, Y. Xiang and A. Tong, *J. Org. Chem.*, 2009, 74, 2163–2166.

12. L. Wang, Y. Xiao, W. Tian and L. Deng, *J. Am. Chem. Soc.*, 2013, **135**, 2903–2906.
13. (a) M. Zhou, Z. Diwu, N. Panchuk–Voloshina and R. P. Haugland, *Anal. Biochem.*, 1997, **253**, 162–168; (b) M. G. Choi, S. Cha, J. E. Park, H. Lee, H. L. Jeon and S. K. Chang, *Org. Lett.*, 2010, 12, 1468–1471; (c) F. Huo, L. Wang, Y. Yang, Y. Chu, C. Yin, J. Chao, Y. Zhang, X. Yan, A. Zheng, S. Jin and P. Zhi, *Analyst*, 2013, **138**, 813–818.
14. C. D. Warren and J. Alroy, *J. Vet. Diagn. Invest.*, 2000, **12**, 483–496.

